IJAMB
INTERNATIONAL JOURNAL OF ADVANCES IN MEDICAL BIOTECHNOLOGY

Effects of calcium phosphates incorporation on structural, thermal and drug–delivery properties of collagen: chitosan scaffolds

Mirella Romanelli Vicente Bertolo[1], Virgínia Conceição Amaro Martins[2], Ana Maria de Guzzi Plepis[3]
**Corresponding author: E–mail address: mirellarvb@gmail.com*

Abstract: In this study, we evaluated how different procedures of calcium phosphate synthesis and its incorporation in collagen:chitosan scaffolds could affect their structural and thermal properties, aiming the obtention of homogeneous scaffolds which can act as drug delivery vehicles in bone tissue engineering. Therefore, three different scaffold preparation procedures were developed, changing the order of addition of the components: in CC–CNPM1 and CC–CNPM2, calcium phosphate synthesis was performed in situ in the chitosan gel (1%, w/w) followed by mixture with collagen (1%, w/w), with changes in the reagents used for calcium phosphate formation; in CC–CNPM3 procedure, calcium phosphate was synthesized *ex situ* and then incorporated into the collagen gel, in which chitosan in powder was mixed. In all procedures, 5% (in dry mass) of ciprofloxacin was incorporated. FTIR analysis confirmed the presence of calcium phosphate in all scaffolds. DSC curves showed that collagen denaturation temperature (Td) increased with calcium incorporation. SEM photomicrographs of scaffolds cross–section revealed porous scaffolds with calcium phosphate grains internally distributed in the polymeric matrix. XRD diffractograms indicated that the calcium phosphates obtained are hydroxyapatite. The pore size distribution was more homogeneous for CC–CNPM3, which also stood out for its smaller porosity and lower absorption in PBS. These results indicate that the *in situ* or *ex situ* phosphate incorporation in the scaffolds had a great influence on its structural properties, which also had consequences for ciprofloxacin release. CC–CNPM3 released a smaller amount of antibiotic (30%), but its release profile was better described by all the tested models.

Keywords: Calcium phosphate; Collagen; Chitosan; Bone Regeneration; Ciprofloxacin Release.

Introduction

Tissue engineering is an interdisciplinary field of sciences which uses principles and methods from engineering, biology, chemistry and physics in order to replace, keep or increase biological functions of tissues or damaged organs.[1] Tissue engineering studies aim to eliminate some of the main disadvantages of conventional clinical treatments, such as high cost, excessive recovery time and possibility of infections.

One of the major areas of tissue engineering is the bone tissue engineering. Bones consist of inorganic compounds such as calcium hydroxy phosphate ($Ca_5(PO_4)_3OH$), also known as hydroxyapatite (HA), calcium carbonate, as well as small quantities of bicarbonate, citrate, magnesium, potassium and traces of other metals. All this inorganic composition represents 65% of bone. 25% is composed of organic compounds as collagen type I, proteoglycans, carbohydrates, besides other proteins. The 10% left correspond to water.[2]

Bone regeneration involves the selection and migration of osteoprogenitors cells, followed by their proliferation, differentiation, matrix formation and bone remodulation.[3] Due to the many *in vitro* steps involved in the process, numerous variables can affect it, such as pH, fluid flow, mechanic and biochemical stimuli, culture medium, temperature, immunologic and inflammatory process, enzymes, as well as number, origin, mobility and activity from cells.[3,4] For this reason, the latest studies in tissue engineering focus on the development of biomaterial–based scaffolds capable of absorbing and releasing bioactive compounds and drugs, besides accelerating the healing response and promoting proper tissue formation.[4]

Scaffolds have been widely used in bone regeneration as a support throughout the recovery process, mimicking the porous architecture of the bone.[5] Besides the support, scaffolds must promote tissue growing, nutrients transport, oxygen diffusion and integration with the host bone, presenting a good biocompatibility with the osteoblasts. During the structural development of the scaffolds, mechanical and biological properties as porosity, pores size, water absorption, mechanical strength and pores shape need to be evaluated and controlled, as they will dictate the ability of the developed material to be applied as an implant or bone substitute.[6,7]

Among the main materials used in the development of scaffolds are natural polymers such as chitosan and collagen, as well as ceramics and minerals needed to mimic the structure and composition of a natural bone.[8,9] Calcium phosphates are one of the most widely used, as they have properties such as nontoxicity, noninflammatory response, and the ability to bind directly to the host bone.[10] Moreover, calcium phosphates as hydroxyapatite can be used in implants and as bone substitutes due its excellent biocompatibility, bioactivity, affinity to biopolymers and osteoconductivity.[11,12] These phosphates can be prepared in many forms, as a dense ceramic, in powder, in particles of micrometric or even nanometric size, according to their applications.[13] HA as nanometric particles has a similarity with the morphology of mineral grains found in bone. Nanometric particles have a greater surface area in relation to volume, which causes an increase in proteins absorption and cellular adhesion in the scaffolds and improves biological and mechanical properties.[14]

Regarding to the natural polymers, the applicability of collagen in tissue engineering brings advantages as its excellent biocompatibility, biodegradability and cellular adhesion properties.[9] In addition, as al–

[1] PhD student in Analytical and Inorganic Chemistry in the postgraduate program in Chemistry at the Institute of Chemistry of São Carlos (IQSC), University of São Paulo (USP).
[2] Chemistry Institute of Chemistry of São Carlos.
[3] Professor at the University of São Paulo, Institute of Chemistry of São Carlos (USP), Department of Chemistry and Molecular Physics.

Received 22 July 2019; Accepted 18 August 2019; Available online 21 September 2019
DOI: https://doi.org/10.25061/2595–3931/IJAMB/2019.v2i2.32

ready mentioned, type I collagen is the most abundant protein in the extracellular matrix of bone, which justifies its widespread use in bone tissue engineering. Many studies have already involved the development of scaffolds, composites and other types of collagen–based materials, associating them with calcium phosphates for bone regeneration: Keeney et al. (2010),[15] developed collagen and calcium phosphate scaffolds as vectors of plasmid DNA transfer; Inzana et al. (2014),[16] developed a 3D printing study of scaffolds based on collagen and calcium phosphate, characterizing them in relation to their cytocompatibility and cell viability.

However, this field still has limitations related to collagen–scaffolds faster degradation and weaker mechanical properties than natural bone.[17] To minimize these disadvantages, some effort has been concentrated in the development of collagen chemically reticulated and/or combined with natural and synthetic polymers. In this sense, the addition of a polymer such as chitosan to the scaffold is an alternative due its biocompatibility, biodegradability, plasticity, adhesiveness and osteoconductive properties.[13] For an example, Zugravu et al. (2012)[5] developed scaffolds based on chitosan/collagen/calcium phosphate microparticles, evaluating the advantages brought by the association of collagen with chitosan over ***in vitro*** compatibility and material biodegradability.

Besides obtaining the scaffolds, one of the biggest problems in surgical interventions is related to the possibility of infections, what takes to the systemic use of antibiotics. Antibiotics administration involves toxicity and a high incidence of antibiotic resistance.[18,19] To avoid these problems a rational use of these drugs is required, avoiding excess or yet the local use instead of systemic treatments. So, a release system that controls the antibiotic rate and keeps its therapeutic concentration during a long period is an advantage over the conventional methods.

To the best of our knowledge, despite numerous reports in the literature on the development of scaffolds and other types of collagen, chitosan and calcium phosphate–based materials, there is no study evaluating different procedures for the incorporation of calcium phosphate salts in the polymer matrix. The order–of–addition of component materials should have effects on the structural properties such as porosity and pore size, thermal properties such as collagen denaturation temperature and the ***in vitro*** antibiotic release, all of them evaluated in this study. We also model the release curves of ciprofloxacin, evaluating the release kinetics.

Materials And Methods

Materials

All solvents and reagents were of analytical grade and used without further purification. The bovine tendon used for collagen extraction was obtained at Casa de Carnes Santa Paula, São Carlos – SP. ***Doryteuthis*** spp. squid pens were obtained at Miami Comércio e Exportação de Pescados Ltda in Cananéa–SP and used as source of β–chitin for chitosan preparation.

Methods

Collagen obtention

To obtain collagen, tendon bovine was treated in an alkaline solution containing salts (chlorides and sulfates of Na^+, K^+ and Ca^{2+}) for 72 h at 25°C, according to the procedure described by Horn et al. (2009).[20] The excess salts were removed by washing in solutions of boric acid (H_3BO_3) and deionized water, followed by washings in EDTA solution and deionized water. Collagen was extracted in pH 3.5 acetic acid (HAc) solution. Collagen gel concentration of 0.98 ± 0.23% was determined by lyophilization.

Chitosan obtention

Chitosan was prepared from squid pens (***Doryteuthis*** spp.) following the procedure of deproteinization and deacetylation adapted from Horn et al. (2009).[20] The reaction yield was 27.8%, which agrees with a previous study.[21] For chitosan characterization, its acetylation degree (6.7%)[22] was determined in a previous study by proton nuclear magnetic resonance spectroscopy (^{1}H NMR), according to the method developed and validated by Lavertu et al. (2003).[23] Chitosan molecular weight (327 kDa)[22] was also previously determined by capillary viscosimetry procedure, according to Rinaudo (2006).[24] 1% (w/w) chitosan gel was obtained in a 1% (w/w) HAc solution, under stirring for 24 h.

Preparation of collagen:chitosan:calcium phosphate scaffolds

In this study, three different procedures for calcium phosphate synthesis and incorporation in collagen and chitosan scaffolds were developed, by changing the reagents used, the order of addition of scaffold components and the ***in situ*** or ***ex situ*** synthesis of phosphate. In all of them, the collagen:chitosan ratio was kept in 1:1 and the amount of calcium phosphate incorporated was the same (35% in relation to the total dry mass of the polymers), being controlled by the molarity and the volume of reagents added in the system. The three procedures developed are described as following:

Procedure 1 (CC–CNPM1)

$CaCl_2$ and $(NH_4)_2HPO_4$ at the concentrations of 0.2 mol L^{-1} and 0.12 mol L^{-1}, respectively, were added in the 1% (w/w) chitosan gel, followed by stirring for 24 h. The pH was raised to 9.0 with 1.0 mol L^{-1} NH_4OH and the stirring kept for more two days. Excess salts of material were removed with water and the chitosan containing the calcium phosphate synthesized was solubilized in HAc solution pH 3.5.

Procedure 2 (CC–CNPM2)

A 0.3 mol L^{-1} solution of H_3PO_4 was added in the 1% (w/w) chitosan gel (in HAc) under constant stirring. Then, a 0.5 mol L^{-1} $Ca(OH)_2$ ethanolic solution was slowly dropped in the mixture, keeping the pH 9.0 for two days. Excess salts of material were removed with water and the chitosan containing the synthesized calcium phosphate was solubilized in HAc solution pH 3.5.

In the two procedures described above, the material obtained ***in situ*** synthesis of calcium phosphate in chitosan was added to the collagen gel (1% w/w, in HAc pH 3.5) and kept under stirring for two days, in order to obtain homogeneous mixtures. The air was removed from the samples, which were placed in Teflon® molds, frozen and freeze–dried. The scaffolds obtained were washed in phosphate buffer saline (PBS) pH 7.4 and in deionized water, frozen and lyophilized.

Procedure 3 (CC–CNPM3)

Nano–calcium phosphate (NCP) was synthetized according to the procedure described by Gopi et al. (2015).[10] In brief, 0.05 mol L^{-1} $CaCl_2.2H_2O$ was added to a 0.15% pectin solution, under stirring for 1 h. 0.03 mol L^{-1} $(NH_4)_2HPO_4$ was dropped into the mixture, under vigorous stirring for 3 h. The pH was adjusted to 9.0 with 1.0 mol L^{-1} NH_4OH, and after 24 h the white precipitate was dried at 80°C, washed with deionized water and ethanol. Finally, calcination eliminated the pectin matrix, ensuring that the powder obtained was only calcium phosphate.

The synthesized calcium phosphate was added to the 1% (w/w) collagen gel (in HAc pH 3.5), keeping the same ratio of the calcium phosphates incorporated on scaffolds of Procedures 1 and 2 (35%). The mixture was kept under stirring for 60 min. Chitosan powder was then added to the mixture, kept under stirring for another 24 h. Thus, this procedure changed not only calcium phosphate ***ex situ*** synthesis, but also the order of salt addition, being initially added to collagen for later incorporation of chitosan powder (and not chitosan gel, as in the other procedures).

The resultant mixture was placed in Teflon® molds, frozen and freeze–dried. The scaffolds were washed in PBS pH 7.4 and in deionized water, frozen and lyophilized.

Ciprofloxacin incorporation

Once the three procedures for obtaining the scaffolds were developed, the antibiotic ciprofloxacin was incorporated into the mixtures. To this end, about 15 g of the mixtures were separated before being frozen

and lyophilized, and to this amount of material 5% (w/w, relative to the dry mass of the polymers) of ciprofloxacin powder, corresponding to 7.5 mg, was added. Thus, the final antibiotic concentration in relation to the collagen:chitosan:calcium phosphate mixture was 0.5 mg g^{-1}. These new mixtures were homogenized by stirring, placed in Teflon® molds, frozen and lyophilized. Scaffolds were neutralized in ammonium vapor for 24 h and aerated under constant air flow for 72 h, being denominated CC–CNPM1–C, CC–CNPM2–C and CC–CNPM3–C.

Fourier transform infrared spectroscopy (FTIR)

CC–CNPM1, CC–CNPM2 and CC–CNPM3 samples were diluted in HAc pH 3.5 (in the ratio of 1:3), placed in Teflon® molds and dried under air flow, in order to form films by the casting method. The spectra were obtained in a FTIR Shimadzu IR Affinity – 1 at a 400 a 4000 cm^{-1} interval with 4 cm^{-1} of resolution.

Thermal stability

Denaturation temperature of collagen present in the scaffolds was obtained by differential scanning calorimeter (DSC) in N_2 atmosphere using a DSC–2010 (TA Instruments). A sample of 20 mg was used, and the heating rate was 10°C min^{-1}, with a temperature range from 5 to 120°C. For the quantification of residue in the scaffolds, thermogravimetric curves (TG) were obtained with a TGA–Q50 (TA Instruments). A sample of 10 mg was used, with a heating rate of 10°C min^{-1} and the temperature range was from 25°C to 800°C, under synthetic air atmosphere.

Scanning electron microscopy (SEM)

The scaffolds morphology was observed using a ZEISS LEO 440 (Cambridge, England) equipment, with an OXFORD detector (model 7060) and an electron beam of 20 kV. Before the analysis, the scaffolds were affixed in stubs with conductive carbon tape and covered with a 6 nm gold layer. The software UTHSCSA Image Tool was used to measure the scaffolds pores. For each one, 20 measures were performed.

X–rays diffraction (XRD)

X–rays diffraction provides a better understanding of the size and nature of synthesized calcium phosphate grains, checking for the presence of crystalline structures in the scaffolds developed. The analysis was performed using monochromatic radiation of CuK, 1,5406 Å, 50 kV, scanning speed of 2° min^{-1} and 2θ between 5 and 80°. Using the diffractogram and the Scherrer's equation (1),[25] the crystal size was calculated:

$$L_{002} = \frac{K\,\lambda}{\beta \cos\theta} \quad (1)$$

In this equation, K is a constant related to the grain size, being its value close to the unitary; λ is the x–ray radiation wavelength (nm); β is the widening of the diffraction peak 002, measured at half the maximum peak intensity, in radians, and θ is the Bragg diffraction angle, in degrees.

Porosity

Scaffold porosity was determined in quintuplicate, according to the procedure described by Nwe et al. (2009).[6] Scaffolds were soaked overnight in water; tissue papers were dried overnight, and their weights were measured. The wet scaffolds had their diameter and thickness measured, so their volume could be calculated. They were placed on the top of the tissue papers and centrifuged at 4,500 rpm for 5 min. The mass of the wet tissue papers was measured, and then the volume of the water absorbed by the scaffold was determined. The porosity was calculated by the relation between this volume (V_2) and the volume of each scaffold (V_1), according to Equation (2).

$$Porosity\ (\%) = \left(\frac{V2}{V1}\right) x\ 100 \quad (2)$$

Absorption in PBS

The study of scaffolds absorption in PBS pH 7.4 was performed in quintuplicate. The dried scaffolds were weighted, placed in PBS buffer and reweighted at specific times. At the end, the percentage of buffer absorbed by each scaffold was calculated using Equation (3).

$$\%\ PBS\ absorbed = \left(\frac{mw - md}{md}\right) x\ 100 \quad (3)$$

Where m_w is the mass of the wetted scaffold, in specific times, and m_d is the initial mass of dried scaffold.

Ciprofloxacin release

The ciprofloxacin release study was made in quintuplicate, by the immersion of scaffolds in 100 mL of PBS pH 7.4, under 100 rpm of stirring and at 37°C. In specific time intervals, aliquots of 1.0 mL were collected, being replaced by 1.0 mL of PBS. Absorbance was read at 271 nm, using a UV spectrophotometer (model HITACHI U–3000).

Statistical analysis

The Shapiro–Wilk test was used to verify data distribution. Pore sizes and porosity results were examined using analysis of variance (ANOVA), followed by Tukey's test. Significance level was set at 5 % in all cases.

Results And Discussion

All scaffolds obtained were porous, homogeneous and white in color, without visible calcium phosphate precipitates. The presence of ciprofloxacin antibiotic did not bring visible changes in the appearance of scaffolds.

Fourier transform infrared spectroscopy (FTIR)

FTIR analysis aims to verify the presence of calcium phosphate characteristics bands in the samples, the first of a series of analysis that allow the confirmation of its incorporation in the scaffolds by the tested procedures. In addition, it can also endorse the presence of typical bands of the polymers used as the scaffolds matrix (collagen and chitosan). FTIR spectra of the samples (CC–CNPM1, CC–CNPM2 and CC–CNPM3) and of the calcium phosphate used in Procedure 3 are shown in Fig. 1.

The spectrum of calcium phosphate confirmed the presence of several characteristics bands: the band at 560 cm^{-1} refers to the deformation of P–O bond in the phosphate group (PO_4^{2-}), while the band at 1041 cm^{-1} is related to P–O stretching.[26] The same phosphate bands (560 and 1041 cm^{-1}) were present in the scaffolds spectra, which also presented large bands at 3300 cm^{-1} referring to the O–H deformation, and characteristics bands of the polymers (collagen and chitosan), as observed at 1630 cm^{-1}, 1540 cm^{-1} and 1230 cm^{-1} (amides I, II and III, respectively).[27] At 1410 and 1450 cm^{-1} can also be observed bands referring to the carbonate group (CO_3^{2-}), usually present in calcium deficient hydroxyapatites as a form of charge compensation.[28] All spectra were similar to each other, with no emphasis on any bands that emerged or differentiated between them.

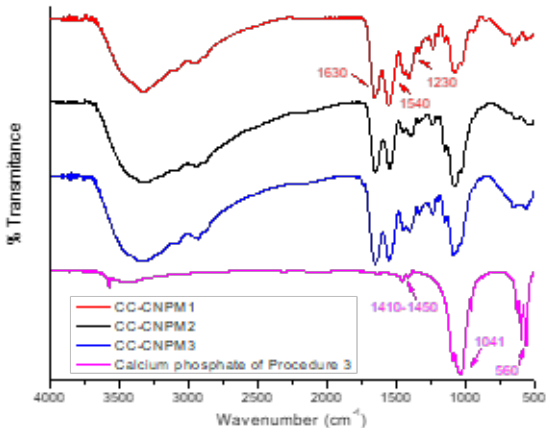

Figure 1 – FTIR spectra of CC–CNPM1, CC–CNPM2, CC–CNPM3 and of the calcium phosphate used in Procedure 3.

Thermal stability

The denaturation temperature (Td) obtained by DSC are presented in Table 1. The analysis was also performed for collagen used in the preparation of scaffolds, and its Td was determined to be 44.8°C. According to Table 1, it is possible to observe an increase in the values in relation to this collagen, which indicates that the calcium phosphate incorporation increased collagen thermal stability, requiring more than 63°C to denature its triple helix.[29]

Thermogravimetric curves for CC–CNPM1, CC–CNPM2 and CC–CNPM3 revealed similar profiles, as shown in Fig. 2. Three stages of weight loss can be observed: from 25 to 200°C, the loss of structural water takes place; the second stage, from 200 to 400°C, is related to the thermal degradation of the collagen structure; finally, the third step refers to the components decomposition and carbonization (400–700°C).[29] Slight differences can be observed in each one of the steps. In general, it is observed that the CC–CNPM1 presented the lowest mass loss values in these three steps.

Furthermore, in all cases it can be observed residues at 700°C related to inorganic components of the scaffolds, especially the calcium phosphate which does not decompose in this temperature range.[30] As shown in Fig. 2, calcium phosphate shows a slight loss of water at the beginning of its curve and remains stable without decomposition over almost the entire working temperature range. Comparing the residual values found for the scaffolds, it can be said that CC–CNPM1 stood out with the highest calcium phosphate content, almost the double of the scaffolds obtained by the other procedures. Thus, it is believed that Procedure 1 generated the largest amount of calcium phosphate in its synthesis *in situ*. Thermogravimetry may have been a first indication of the influence of the different adopted procedures on the properties of the obtained scaffolds.

Scaffold	Td (°C)	Weight loss (%)			Residue (%)
		25–200°C	200–400°C	400–700°C	700°C
CC–CNPM1	65.5	9.9	30.3	14.9	44.8
CC–CNPM2	63.8	17.1	38.1	23.6	20.9
CC–CNPM3	67.9	10.5	37.0	29.0	22.5

Table 1 – Thermal parameters and residue content at 700°C of CC–CNPM1, CC–CNPPM2 and CC–CNPM3 scaffolds.

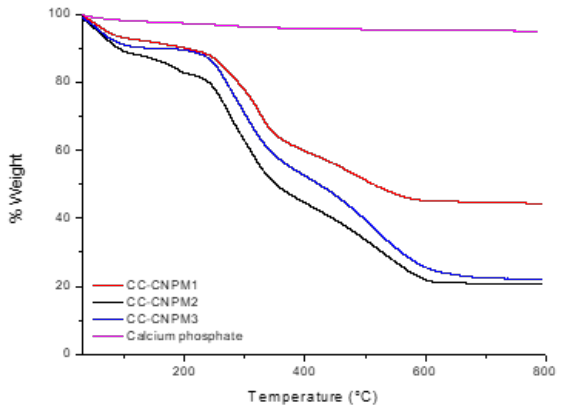

Figure 2 – Thermogravimetric curves for CC–CNPM1, CC–CNPM2, CC–NPM3 and synthesized calcium phosphate.

Scanning electron microscopy (SEM)

The photomicrographs obtained by SEM are shown in Fig. 3. The scaffolds were porous, with calcium phosphate grains internally distributed throughout the polymer matrix and no larger than 300 nm. However, differences can be observed regarding the quantity and size of scaffold pores, as well as regarding the morphology of the grains and their quantity.

From Fig. 3A, 3C and 3E, all with the same magnification (25,000x), there is a distinct difference with respect to the morphology of the scaffolds: although CC–CNPM3 presents itself as a more compact scaffold and its pores are more homogeneous and better distributed, the same does not occur in CC–CNPM2, in which no well–defined pores are observed.

Regarding to calcium phosphate (Fig. 3B, 3D and 3F), the formed grains are clearly different from each other. In CC–CNPM1, their needle–like shape resembles CC–CNPM3 grains, but in the latter case they are smaller and better distributed along the scaffold cross section. Li et al. (2010)[31] reported obtaining needle–shaped apatite formed on the chitosan surface after a mineralization process by immersion in saline solutions. However, the grains obtained by them were about 7 times larger than the calcium phosphates formed in CC–CNPM1. On the other hand, the calcium phosphate grains in CC–CNPM2 are spherical in shape, aggregated and poorly distributed in the scaffold. The same spherical shape of calcium phosphates can be observed in the work of Zhao et al. (2008),[32] who mineralized scaffolds based on collagen and chitosan, obtaining calcium phosphates of different shapes and sizes, according to the calcium ion concentration.

ImageJ software was used to measure the size of scaffold pores using SEM photomicrographs with 500x of magnification. Table 2 shows the average surface and cross–sectional pore size of the scaffolds. In general, all samples presented at least 40% of their surface pores with sizes that varied within the same range, which were larger for CC–CNPM2 (between 30 and 40 µm) than for the other two cases (Fig. 4).

CC–CNPM3 presented smaller surface and cross–sectional pores, with approximately the same size range (5 to 40 µm), unlike CC–CNPM1 in which the cross–sectional pores were almost twice the average pore size of the surface pores. On the other hand, CC–CNPM2 showed a more heterogeneous pore size distribution, both at surface (range 10 to 65 µm) and cross sectional (range 10 to 55 µm). Thus, from the analysis of SEM images and of the surface and cross–sectional pores of the samples, it can be concluded that the ***ex situ*** calcium phosphate incorporation adopted in CC–CNPM3 was the procedure that resulted in more homogeneous scaffolds with better defined pores.

According to Karageorgiou & Kaplan (2005),[33] pores with sizes around 100 µm are favorable for cell growth and nutrient transport. Although the scaffolds developed by the three procedures presented pore sizes smaller than 100 µm, studies involving ***in vitro*** evaluation of osteoblasts growth in collagen scaffolds with smaller pores have already been successfully conducted.[34]

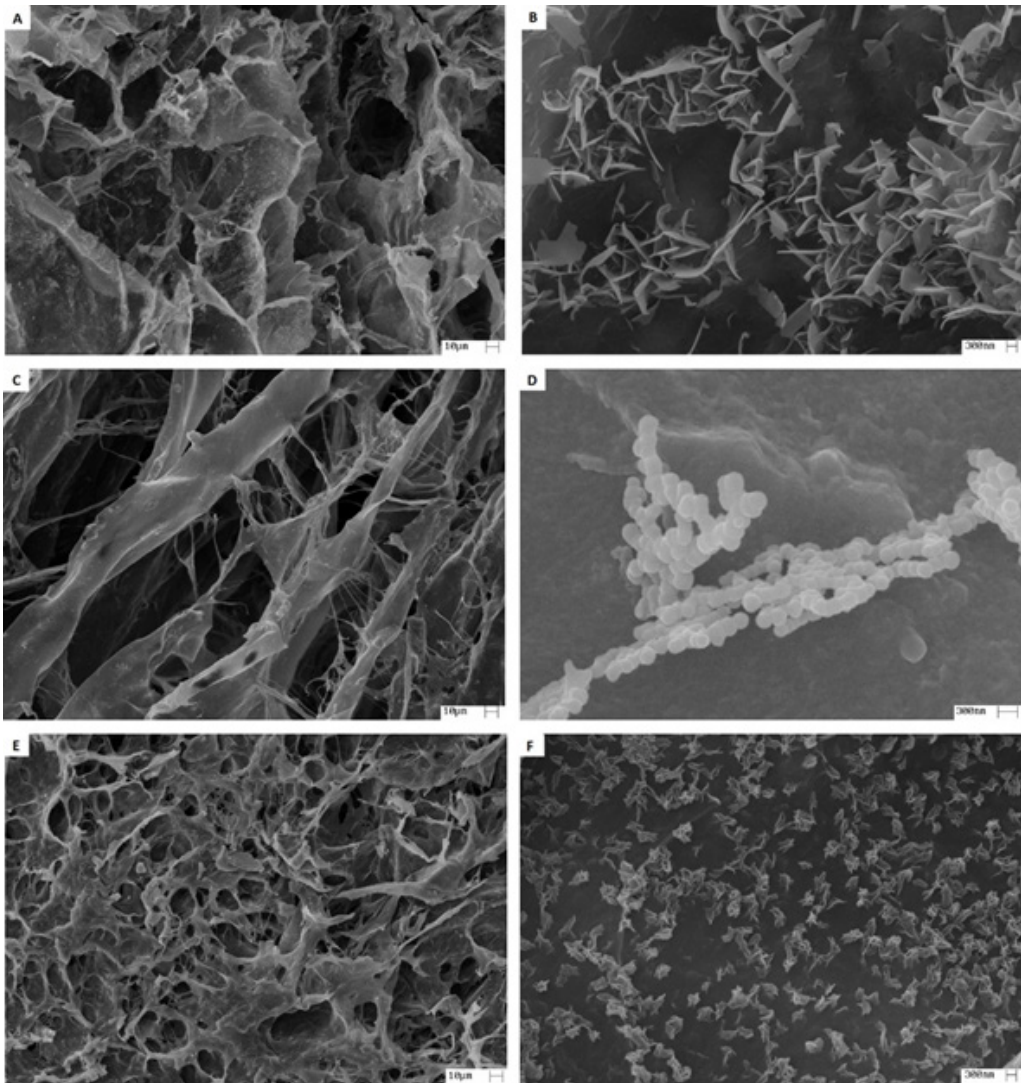

Figure 3 – Photomicrographs by SEM of cross section of: (A) and (B) CC–CNPM1, (C) and (D) CC–CNPM2, (E) and (F) CC–CNPM3. Magnitude of 1,000x (A), (C) and (E); 25,000x (B) and (F); 30,000x (D).

Scaffold	Pores sizes ± SD (μm)	
	Surface	Cross–section
CC–CNPM1	17.7 ± 6.8[b]	42.8 ± 9.2[a]
CC–CNPM2	38.2 ± 14.3[a]	31.2 ± 13.7[b]
CC–CNPM3	21.1 ± 8.5[b]	18.4 ± 8.7[c]

In the same column, values with the same superscript letter (a–b) were not significantly different ($P > 0.05$).

Table 2 – Pores sizes by SEM photomicrographs for CC–CNPM1, CC–CNPM2 and CC–CNPM3 scaffolds.

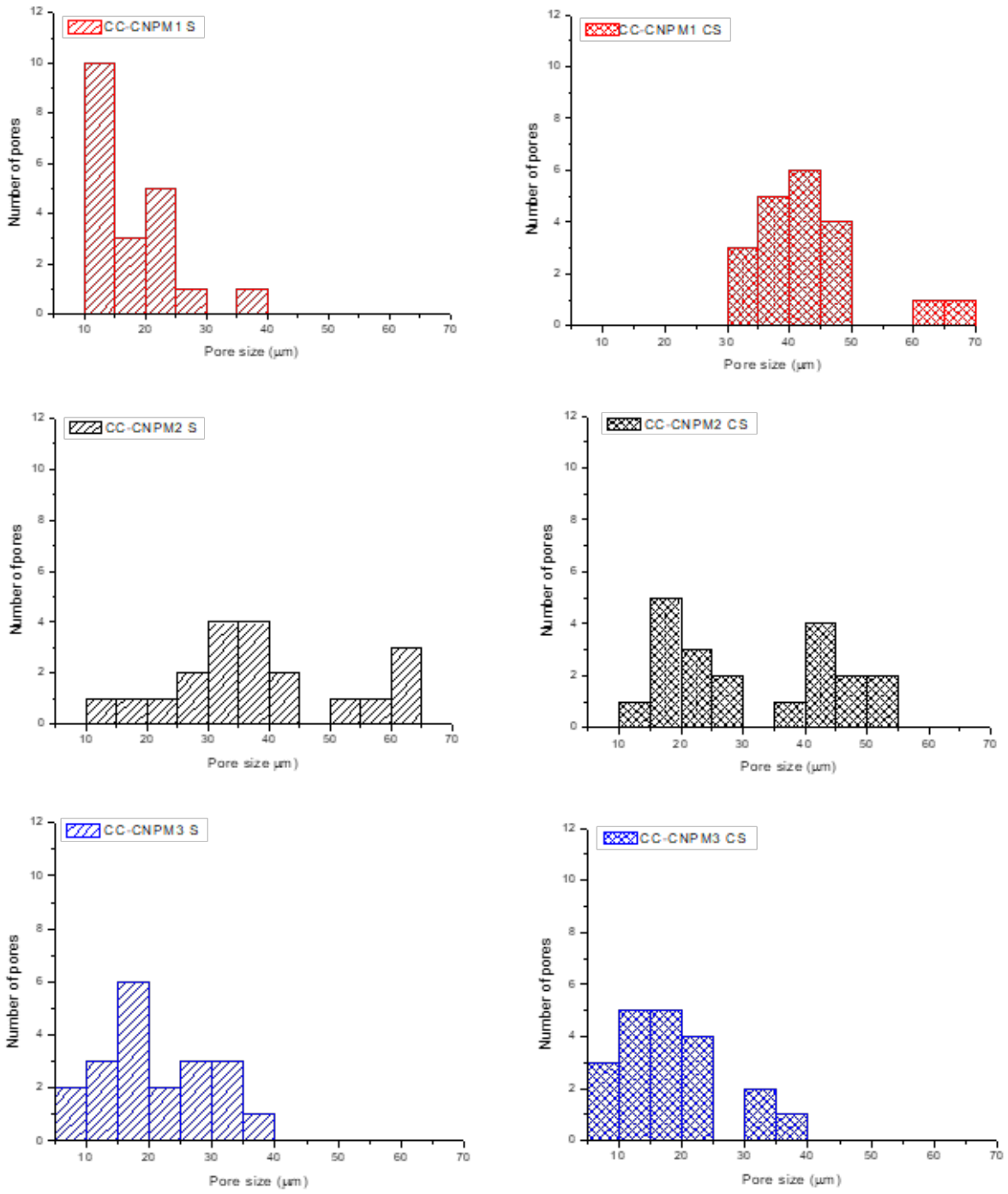

Figure 4 – Histograms of pore size distribution for surface (S) and cross–sectional (CS) SEM images.

X-rays diffraction (XRD)

X-rays diffraction analysis was performed to identify the crystalline phases present in the scaffolds developed, as well as in the calcium phosphate synthesized *ex situ* for Procedure 3 (Fig. 5).

As can be seen in Fig. 5, the peaks at 2θ=32° characteristic of the (211) plane of hydroxyapatite[35] appear in all diffractograms presented, with greater intensity and better resolution in the case of isolated calcium phosphate diffractogram. The well-marked peaks confirm that the calcium phosphates obtained in the procedures developed is this study are believed to be hydroxyapatite.

In the scaffold spectra, the presence of collagen and chitosan interferes with the crystallinity of the mineral content. Zugravu et al. (2012),[5] studied the effects of different collagen concentrations on the calcium phosphate crystallinity incorporated in composite microparticles. They reported that at a 25% collagen concentration, calcium phosphate peaks completely disappeared from the spectra. Furthermore, in the scaffold spectra two additional peaks can be observed, at 2θ=10° and 2θ=20°, referring to the chitosan hydrous and anhydrous peaks, respectively.[35]

The grain size of HA synthesized in Procedure 3 was measured by the enlargement of diffraction peak 002, indicated in the spectrum. Scherrer equation's (1) was used to calculate the grain size, and the value obtained was 21.4 nm, which confirms HA synthesis in nanometric dimensions.

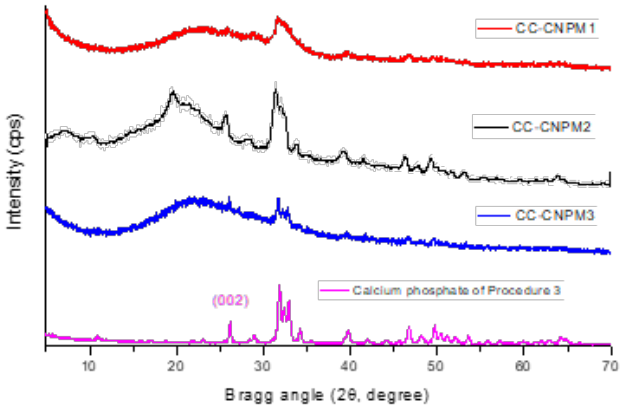

Figure 5 – Representative XRD spectra of collagen/chitosan/calcium phosphate scaffolds compared to the calcium phosphate synthesized in Procedure 3.

Scaffolds porosity and absorption in PBS

Scaffolds porosity, in addition to pores size and morphology, is an essential factor to be studied when considering the application of these materials in bone regeneration, as it influences processes such as water absorption, PBS absorption, migration and cell growth. Table 3 shows the porosity values obtained for the developed scaffolds, as well as their relative absorption percentage in PBS pH 7.4.

It can be observed from the porosity values presented that, although there are no significant statistical differences between the procedures, the scaffolds obtained by Procedures 1 and 2 (*in situ* procedures) showed a tendency to be more porous than the scaffolds prepared by Procedure 3, in which phosphate incorporation was *ex situ*.

PBS absorption study is critical to evaluate whether prepared scaffolds can be used as controlled drug delivery vehicles. Fig. 6 shows the mean absorption curves in PBS as a function of time for CC-CNPM1, CC-CNPM2 and CC-CNPM3 scaffolds.

The percentage of PBS absorbed, as well as the absorption profile, differ between the scaffolds. While CC-CNPM1 and CC-CNPM2 both stabilized in 1,500% or more and in approximately 1 min, CC-CNPM3 stabilized their absorption in 1,100% after 10 min. The absorption results may be related to the scaffold porosity: as seen, CC-CNPM3 was the least porous scaffold among the three developed, and it was expected that its PBS absorption was also the lowest. Nevertheless, all prepared scaffolds absorbed large amounts of buffer over a short period of time, which is a promising result for their use as drug carriers and delivery systems.

PBS absorption and porosity results, when combined with scaffolds pore size distribution data, allow an important conclusion to be drawn as the direction of this study: the order of addition of scaffold components, as well as the way calcium phosphate is incorporated, have a greater influence on the porous structure of the final material than the simple reagents change evaluated in the *in situ* procedures developed. Thus, CC-CNPM3 scaffolds were the least porous and absorbed less PBS but presented a more homogeneous pore distribution and smaller surface and cross-sectional pores. CC-CNPM1 and CC-CNPM2, in turn, despite having different pore size distributions, presented similar porosities and absorption profiles.

Scaffold	Porosity ± SD (%)	% PBS absorbed
CC-CNPM1	30.6 ± 5.3[a]	1,600
CC-CNPM2	30.1 ± 2.7[a]	1,495
CC-CNPM3	23.9 ± 4.8[a]	1,062

In the same column, values with the same superscript letter (a) were not significantly different (P > 0.05).

Table 3 – Porosity and PBS absorption for CC-CNPM1, CC-CNPM2 and CC-CNPM3.

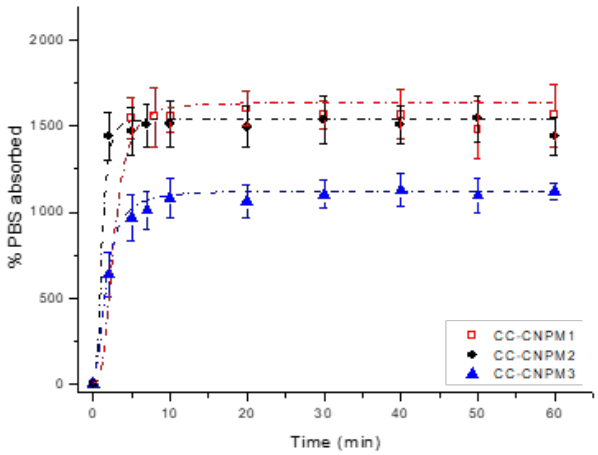

Figure 6 – PBS absorption profiles for CC–CNPM1, CC–CNPM2 and CC–CNPM3.

Ciprofloxacin release

Fig. 7 shows the mean release profile of ciprofloxacin by the scaffolds. As expected, CC–CNPM3–C presented the most distinct profile, releasing approximately 30% (0.4 mg) of their incorporated antibiotic after about 2 h of assay. CC–CNPM1–C and CC–CNPM2–C released 40% (0.45 mg) and 63% (0.7 mg) of their ciprofloxacin, respectively, stabilizing these percentages after about 1 h of assay.

Although the release time was well balanced in all cases and stabilization occurred at acceptable time intervals, the maximum release percentages were relatively low. The reason for this may be related to the structure of ciprofloxacin: the antibiotic is a fluorquinolone, which can complex with calcium ions of phosphate present in scaffolds, making it difficult to release (Fig. 8).[36,37] This fact also explains why CC–CNPM1–C released less antibiotic, despite having a PBS absorption profile similar to CC–CNPM2–C: its inorganic content was the highest, which implies a possible greater complexation between its HA incorporated therein and ciprofloxacin.

Despite the released concentrations are low in relation to the total antibiotic incorporated, depending on the application to which the scaffold is submitted (application site, type of injury) the amount of ciprofloxacin released may still be enough or even higher than the required therapeutic concentration. According to the FDA, the recommended dose of ciprofloxacin to be consumed in a day is 250 to 1000 mg, but a concentration of 2 μg mL^{-1} is already enough to inhibit a huge range of microorganisms, as *E. coli* and *S. aureus*.[38] Thus, all scaffolds developed in this study released larger amounts of ciprofloxacin in a much shorter time period than 24 h.

In order to better understand which drug release mechanisms were involved for each of the prepared scaffolds, different release models were tested, including: first order, second order, Hixson–Crowell, Baker–Lonsdale, Korsmeyer–Peppas, Higuchi and Weilbull.[39,40] Only the three last models showed satisfactory results for the samples developed in this study, and their equations and parameters are described in Table 4.

Table 5 lists the main parameters obtained by modeling the ciprofloxacin release curves for CC–CNPM1–C, CC–CNPM2–C and CC–CNPM3–C samples, according to the three models described above. As can be observed, CC–CNPM3–C was best fitted in all tested models, presenting the highest R values. The release curves of CC–CNPM1–C and CC–CNPM2–C were best adjusted by the Korsmeyer–Peppas model. This model is used in systems in which more than one process is involved in drug release: for samples with $0.5 < n < 1.0$, the drug transport mechanism is called anomalous or non–Fickian, and its release mechanisms can be by diffusion or by relaxation of polymeric chains.[40] Otherwise, if $n < 0.5$ the transport drug mechanism in denominated Quasi–Fickian diffusion, and its kinetics of diffusion is completely different from the non–Fickian mechanism. In this case, it is believed that the polymer chains have more mobility, releasing a greater amount of drug by diffusion than the non–Fickian model would release.

According to Table 5, CC–CNPM1–C and CC–CNPM2–C showed Quasi–Fickian diffusion mechanisms, while CC–CNPM3–C presented a non–Fickian mechanism, releasing ciprofloxacin by diffusion and/or relaxation in the polymeric matrix. Different mechanisms of diffusion were really expected for this sample, since the profile of its release curve was very different from the others (Fig. 7), as well as its maximum amount of ciprofloxacin released. Thus, it can be said that although CC–CNPM3–C was the sample that released the least amount of antibiotic, its release was the most controlled of the three cases, and it would be chosen as the best release model for ciprofloxacin.

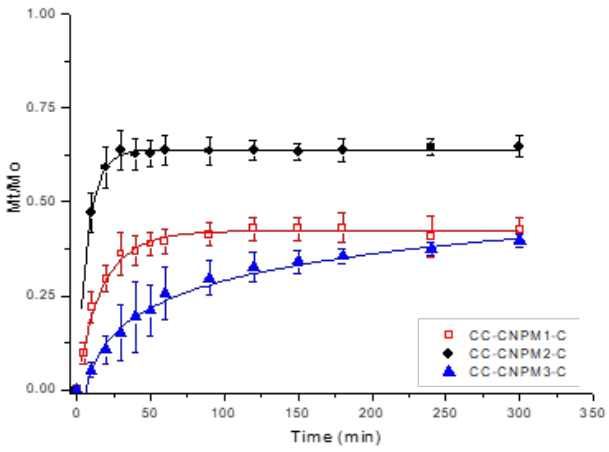

Figure 7 – Ciprofloxacin release profile of the scaffolds. Release conditions: 37°C, 100 rpm, absorbance reading at 271 nm.

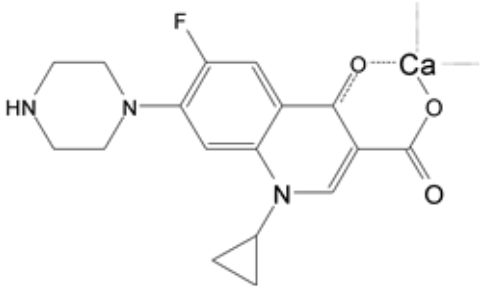

Figure 8 – Complexation between the ciprofloxacin and calcium ions from phosphates.

Model	Equation	Parameter(s)
Higuchi[38]	$Mt/Mo = k.t^{0.5}$	**k** is Higuchi kinetic constant; **Mt** is the amount of drug dissolved in time **t**; **Mo** is the initial amount of drug
Korsmeyer–Peppas[38]	$Mt/Mo = k.t^{n}$ $\ln(Mt/Mo) = \ln(k) + n.\ln(t)$	**k** is Korsmeyer–Peppas kinetic constant, **n** is the release exponent, indicative of the drug release mechanism
Weibull[38]	$\frac{Mt}{Mo} = 1 - e^{-[(t-T)^b]/a}$ $\log[-\ln(1-M\_t/M\_0)] = b.\log(t) - \log(a)$	**T** is the location parameter, represents the lag time before the onset of the dissolution or release process and in most of the cases will be zero; **a** is the scale parameter defines the time scale of the process; **b** shape of dissolution curve as either exponential (b=1), *S*–shaped (b>1) or parabolic (b<1)

Table 4 – Model equations used for fitting ciprofloxacin release data.

Models	Scaffolds		
	CC–CNPM1–C	CC–CNPM2–C	CC–CNPM3–C
Higuchi			
k	0.02136	0.01476	0.03188
R	0.91934	0.87986	**0.98727**
Korsmeyer–Peppas			
k	0.16483	2.89548	0.00986
n	0.21357	0.09724	0.74079
R	**0.95788**	**0.93737**	**0.98087**
Weibull			
a	4.1468	2.04207	60.9116
b	0.16327	0.08449	0.61416
R	0.88836	0.87812	**0.96201**

Table 5 – Parameters obtained by modeling ciprofloxacin release curves for CC–CNPM1–C, CC–CNPM2–C and CC–CNPM3–C.

Conclusion

This study revealed an unprecedented study of the development of three distinct procedures for the synthesis and incorporation of calcium phosphates in collagen and chitosan–based polymeric systems, aiming to obtain homogeneous scaffolds that could act as controlled release vehicles of ciprofloxacin. The materials were structurally characterized, presenting internally distributed calcium phosphate grains and pores of different shapes and size distributions. Studies of scaffolds porosity, pore size and absorption in PBS were conducted, and all results pointed in the same direction: CC–CNPM1 and CC–CNPM2, in which calcium phosphate synthesis occurred ***in situ***, presented porosities and absorption profiles in PBS quite different from CC–CNPM3, in which phosphate incorporation was by simple mixture, confirming that the order of addition of scaffold components actually interferes with their final structural properties. Finally, the release study of ciprofloxacin revealed by modeling the data that CC–CNPM3–C stood out as the sample that released this antibiotic by both diffusion and relaxation of the polymeric matrix, although it released a smaller amount of the drug. It is expected that this study opens new possibilities of application of the developed materials, once some of the main important aspects for their application in the area of bone regeneration have been characterized.

Conflict of Interests

There are no conflicts to declare.

Acnlowledgements

The authors would like to thank the Center of Analytical Chemical Analysis of IQSC/USP, for all the infrastructure available for FTIR, SEM, 1H NMR and XRD analysis. We also thank Prof. Dr. Sérgio Paulo Campana Filho (IQSC/USP) for the access of the viscometer SCHOTT equipment and Prof. Dr. Agnieszka Joanna Pawlicka Maule (IQSC/USP) for the access of the TGA–Q50 instrument (FAPESP grant number 2010/19417–0).

Funding

This study was supported by the National Council for Scientific and Technological Development (CNPq) contract number 148856/2016–0.

References

1. Lanza R, Langer R, Vacanti J, Principles of Tissue Engineering. *Academic Press*, New York, NY, USA, 3rd edition (2007).
2. Wojnar R, Bone and Cartilage – its Structure and Physical Properties. *Biomechanics of Hard Tissues: Modeling, Testing, and Materials*, ed. by Andreas Ochsner e Waqar Ahmed, WILEY–VCH Verlag GmbH & Co. KGaA, Weinheim, Germany (2010).
3. Velasco MA, Narváez–Tovar CA, Garzón–Alvarado DA, Design, Materials, and Mechanobiology of Biodegradable Scaffolds for Bone Tissue Engineering. *BioMed Res Int*, **2015** :729076, (2015).
4. Fisher MB, Mauck RL, Tissue Engineering and Regenerative Medicine: Recent Innovations and the Transition to Translation. *Tissue Eng Part B Rev*, **19** :1–13 (2013).
5. Zugravu MV et al., Physical properties and in vitro evaluation of collagen–chitosan–calcium phosphate microparticle–based scaffolds for bone tissue regeneration. *J Biomed Appl*, **28(4)** :566–579 (2012).
6. Nwe N, Furuike T, Tamura H, The mechanical and biological properties of chitosan scaffolds for tissue regeneration templates are significantly enhanced by chitosan from *Gongronella butleri. Materials*, **2** :374–398 (2009).
7. Wu S et al., Biomimetic porous scaffolds for bone tissue engineering. *Mat Sci Eng R*, **80** :1–36 (2014).
8. Rodrígues–Vázquez M et al., Chitosan and Its Potential Use as a Scaffold for Tissue Engineering in Regenerative Medicine. *Biomed Res Int*, 821279 (2015).
9. Dong C & Yonggang Lv, Application of Collagen Scaffold in Tissue Engineering: Recent Advances and New Perspectives. *Polymers*, **8(2)** :42 (2016).
10. Gopi D, Kanimozhi K, Kavitha L, *Opuntia ficus indica* peel derived pectin mediated hydroxyapatite nanoparticles: Synthesis, spectral characterization, biological and antimicrobial activities. *Spectrochim Acta, Part A*, **141** :135–143 (2015).
11. Chen DZ et al., Dynamic mechanical properties and *in vitro* bioactivity of PHBHV/HA nanocomposite. *Compos Sci Technol*, **67** :1617–1626 (2007).
12. Pelin IM et al., Preparation and characterization of a hydroxyapatite–collagen composite as component for injectable bone substitute. *Mater Sci Eng C*, **29** :2188–2194 (2009).
13. Elhendawi H et al., Effect of synthesis temperature on the crystallization and growth of in situ prepared nanohydroxyapatite in chitosan matrix. *ISRN Biomaterials*, **2014** :897468 (2014).
14. Ghomi H, Fathi MH, Edris H, Preparation of nanostructure hydroxyapatite scaffold for tissue engineering applications. *J. Sol–Gel Sci Technol*, **58** :642–650 (2011).
15. Keeney M et al., The ability of a collagen/calcium phosphate scaffold to act as its own vector for gene delivery and to promote bone formation via transfection with $VEGF_{165}$. *Biomaterials*, **31** :2893–2902 (2010).
16. Inzana JA et al., 3D printing of composite calcium phosphate and collagen scaffolds for bone regeneration. *Biomaterials*, **35** :4026–4034 (2014).
17. Ferreira AM, Gentile P, Chiono V, Ciardelli G, Collagen for bone tissue regeneration. *Acta Biomater,* **8** :3191–3200 (2012).
18. Nandi SK et al., Local antibiotic delivery systems for the treatment of osteomyelitis: a review. *Mater Sci Eng C*, **29** :2478–2485 (2009).
19. Zhang X et al., Teicoplanin–loaded borate bioactive glass implants for treating chronic bone infection in a rabbit tibia osteomyelitis model. *Biomaterials*, **31** :5865–5874 (2010).
20. Horn MM, Martins VCA, Plepis AMG, Interaction of anionic collagen with chitosan: Effect on thermal and morphological characteristics. *Carbohydr Polym*, **77** :239–243 (2009).
21. Kurita K, Chitin and chitosan: Functional biopolymers from marine crustaceans. *Mar Biotechnol*, **8(3)** :203–226 (2006).
22. Bertolo M et al., Rheological and antioxidant properties of chitosan/gelatin–based materials functionalized by pomegranate peel extract. *Carbohydr Polym*, **228** :115386 (2020).
23. Lavertu M et al., A validated 1H NMR method for the determination of the degree of deacetylation of chitosan. *J Pharm Biomed Anal,* **32(6)** :1149–1158 (2003).
24. Rinaudo M. Chitin and chitosan: Properties and applications. *Prog Polym Sci*, **31** :603–632 (2006).
25. Barrère F, Layrolle P, Van Blitterswijk CA, De Groot K, Biomimetic Calcium Phosphate Coatings on Ti6Al4V: A Crystal Growth Study of Octacalcium Phosphate and Inhibition by Mg^{2+} and HCO_3^-. *Bone*, **25(2)** :107S–111S (1999).

26. Pereda M et al., Chitosan–gelatin composites and bi–layer films with potential antimicrobial activity. *Food Hydrocoll*, **25(5)** :1372–1381 (2011).

27. Batista TM, Martins VCA, Plepis AMG, Thermal behavior of in vitro mineralized anionic collagen matrices. *J Therm Anal Calorim*, **95** :945–949 (2009).

28. Berzina–Cimdina L & Borodajenko N, Research of Calcium Phosphates Using Fourier Transform Infrared Spectroscopy, Infrared Spectroscopy – Materials Science, Engineering and Technology, Prof. Theophanides Theophile (Ed.), ISBN: 978–953–51–0537–4, InTech, 2012.

29. Kanapathipillai M et al., Synthesis and Characterization of Ionic Block Copolymer Templated Calcium Phosphate Nanocomposites. *Chem Mater*, **20** :5922–5932 (2008).

30. Koutsopoulos S. Synthesis and characterization of hydroxyapatite grains: A review study on the analytical methods. *J Biomed Mater Res*, **62(4)** :600–612 (2002).

31. Li B, Huang Y, Wang Y, Zhou Y. Mineralization of Bone–like Apatite in Chitosan Hydrogel. *Key Eng Mat*, **434–435** :605–608 (2010).

32. Zhao H, Ma L, Gao C, Shen J. Fabrication and properties of mineralized collagen–chitosan/hydroxyapatite scaffolds. *Polym Adv Technol*, **19** :1590–1596 (2008).

33. Karageorgiou V & Kaplan D, Porosity of 3D biomaterial scaffolds and osteogenesis. *Biomaterials*, **26(27)** :5474–5491 (2005).

34. Liu LS, Thompson AY, Heidaran MA, Poser JW, Spiro RC. An osteoconductive collagen/hyaluronate matrix for bone regeneration. *Biomaterials*, **20(12)** :1097–1108 (1999).

35. Chesnutt BM et al., Design and characterization of a novel chitosan/nanocrystalline calcium phosphate composite scaffold for bone regeneration. [Evaluation Studies]. *J Biomed Mater Res Part A*, **88(2)** :491–502 (2008).

36. Martins VCA & Goissis G, Nonstoichiometric hydroxyapatite–anionic collagen composite as support for the double sustained release of gentamicin and norfloxacin/ciprofloxacin. *Artif Organs*, **24(3)** :224–230 (2000).

37. Wallis SC et al., Interaction of norfloxacin with divalent and trivalent pharmaceutical cations: in vitro complexation and in vivo pharmacokinetic studies in the dog. *J Pharm Sci*, **85** :803–809 (1996).

38. Kelly DJ et al. Serum concentrations of penicillin, doxycycline, and ciprofloxacin during prolonged therapy in rhesus monkeys. *J Infect Dis*; **166** :1184–1187 (1992).

39. Paarakh MP et al., Release kinetics – concepts and applications. *Int J Pharm Res Technol*, **8** :12–20 (2018).

40. Shaikh HK, Kshirsagar RV & Patil SG. Mathematical models for drug release characterization: a review. *Int J Pharm Pharm Sci*, **4(4)**: 324–338 (2015).